Bulletin of the Seismological Society of America, Vol. 80, No. 2, pp. 483–487, April 1990

SHORT NOTES

THE 3 DECEMBER 1988, PASADENA EARTHQUAKE (M_L = 4.9) RECORDED WITH THE VERY BROADBAND SYSTEM IN PASADENA

BY HIROO KANAMORI, JIM MORI, AND THOMAS H. HEATON

Since 1 December 1987, a very broadband seismographic system has been in operation at the Kresge Laboratory of the California Institute of Technology. This system consists of the Streckeisen-1 very broadband sensor (Wielandt and Streckeisen, 1982), the Kinemetrics FBA-23 triaxial force balance accelerometer and a Quanterra data-logger with a 24-bit (for Streckeisen-1) and a 16-bit (for FBA-23) digitizer. The details of the data logger are described in Steim (1986). The overall dynamic range of this system is about 200 db. This system was constructed as a joint project between the California Institute of Technology, the U.S. Geological Survey, the University of Southern California and the International Research Institution for Seismology (IRIS), and is an element of the IRIS global network as well as the TERRAscope network of California Institute of Technology. A brief description of the system is given by Given *et al.* (1989).

The Very Broadband (VBB) system recorded the 3 December 1988, Pasadena earthquake (Origin Time: 12/3/1988 11:38:26 GMT; M_L = 4.9; 34.1412N, 118.1327W; depth = 15.6 km) on scale. These records are unique because the station is only about 4 km from the epicenter so that not only the far-field but also near-field displacements were clearly recorded. The maximum acceleration at this station was about 5 per cent of g.

Figure 1a shows the displacement trace obtained from the low-gain channel (Kinemetrics FBA-23) by time-domain integration with high-pass filtering at 5 sec to remove the baseline drift. The far-field pulses and the near-field displacement (displacement between P and S) are clearly recorded.

FAR FIELD

We first rotated the N–S and E–W components into the radial and transverse components (Fig. 1b). Both P and S waves exhibit two pulses indicating two distinct sources about 0.4 sec apart. The aftershocks recorded at the same station exhibit a single pulse, which proves that the observed double pulse is caused by the source, and not by the propagation effect.

Since the distance to the hypocenter is very short (Δ = 3.89 km, azimuth = 282.9°, backazimuth = 102.9°), the far-field P and S pulses can be inverted to obtain the source parameters using the method described in Kanamori (1989). In this method, the moment rate function is approximated by a simple triangle and the amplitude and polarity of P, SV, and SH waves are used to determine the seismic moment and the three fault parameters (dip, rake, and strike).

We approximate the double event by two triangles 0.4 sec apart, each 0.4 sec wide. For simplicity, the structure is assumed to be a homogeneous whole space (P velocity = 6 km/sec, S velocity = 3.5 km/sec, density = 2.6 g/cm^3). The free-surface effect is approximated by a factor of 2 amplification of the incidence wave. For near vertical incidence, this approximation is considered satisfactory. Since the

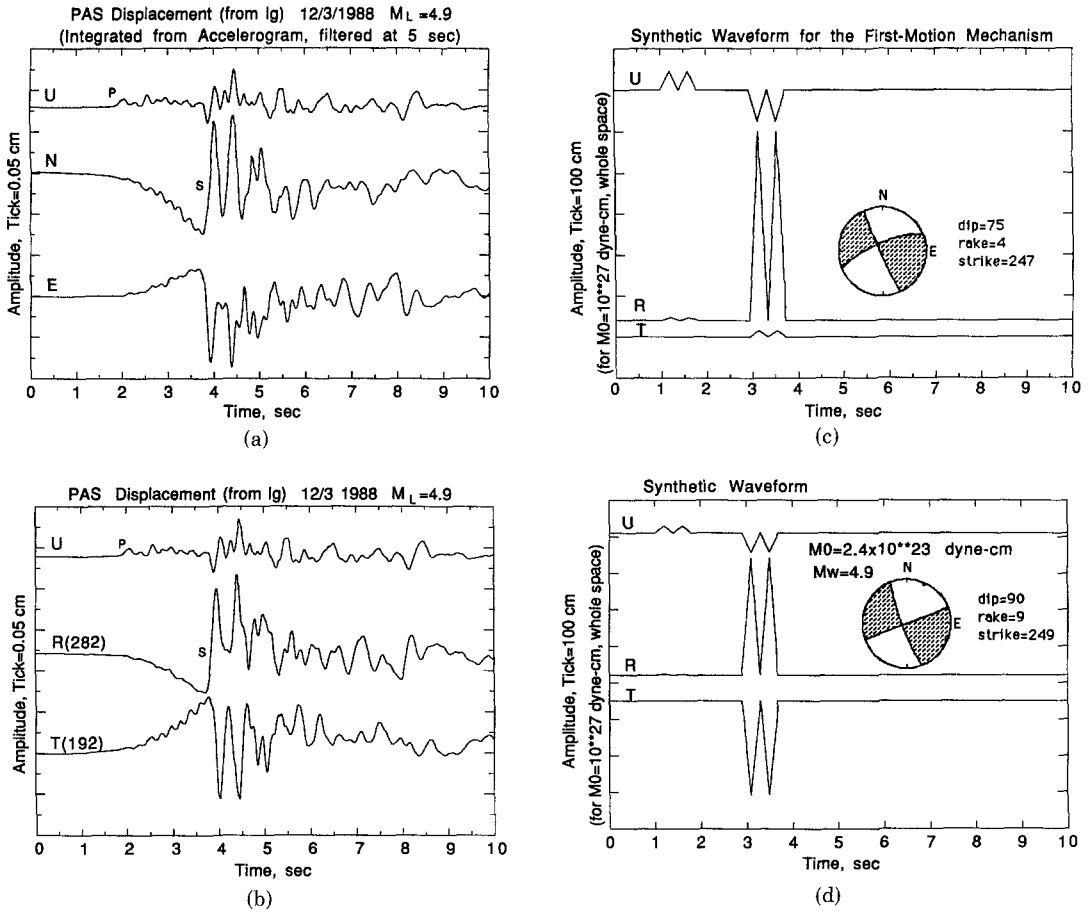

FIG. 1. (a) Displacement records of the 3 December 1988, Pasadena earthquake obtained from the Low-Gain channel of the Pasadena system (high-pass-filtered at 5 sec). (b) Rotated displacement of the 3 December 1988 Pasadena earthquake. (c) The mechanism obtained from the first-motion data and the corresponding far-field synthetics. (d) The mechanism inverted from the displacement records and the corresponding far-field synthetics.

number of parameters (4) is larger than the number of data (3), the solution is non-unique. However, if a first approximation is given, the best solution can be found in its closest neighborhood. We used the mechanism determined from the first-motion data (Jones *et al.*, 1989) as the first approximation. Figure 1c shows the synthetic seismograms for the first-motion mechanism. Note that the *SH* wave is very small and its polarity is opposite to the observed.

Figure 1d shows the mechanism obtained by the inversion and the corresponding synthetics. The amplitude and polarity of the observed seismograms are explained well. The mechanism thus determined is: 1st nodal plane: dip = 90°, rake = 0°, strike = 249°, 2nd nodal plane: dip = 81°, rake = 180°, strike = 159°. The total seismic moment is 2.4×10^{23} dyne-cm ($M_w = 4.9$). Since the location of the Pasadena station is very close to the node of *P*, *SV*, and *SH* waves, a small error in the location can cause considerable errors in the inversion. However, the event was located with more than 50 stations within 100 km and 5 stations within a distance comparable to the focal depth, of which 3 stations had horizontal components with clear *S* waves. The absolute location accuracy of this event is

considered ±0.5 km in the epicenter and ±1 km in the depth. To examine the effect of mislocation on the mechanism, we displaced the epicenter by as much as 1 km and determined the mechanism. The difference in the fault parameters for these different epicenters is less than a few degrees. Hence the fault geometry shown in Figure 1d is considered accurate within a few degrees in dip, rake, and strike.

Near Field

We modeled the near-field displacement (between P and S waves) using Haskell's (1969) method. Figure 2a shows the synthetics computed for a fault model with rise time of 0.2 sec, fault length of 2 km, fault width of 1 km, and unilateral rupture velocity of 2.5 km. The mechanism shown in Figure 1d was used. The overall pattern (the amplitude ratio of the N–S to E–W component) of the observed near-field displacements is explained very well with this model. To match the observed amplitude, a displacement of 76 cm is required on the fault plane (1×2 km^2), which gives a seismic moment of 4.6×10^{23} dyne-cm ($M_w = 5.0$). This value is about a factor of 2 larger than that obtained from the far-field pulses. This difference is not surprising considering that significant ground motions follow the two pulses

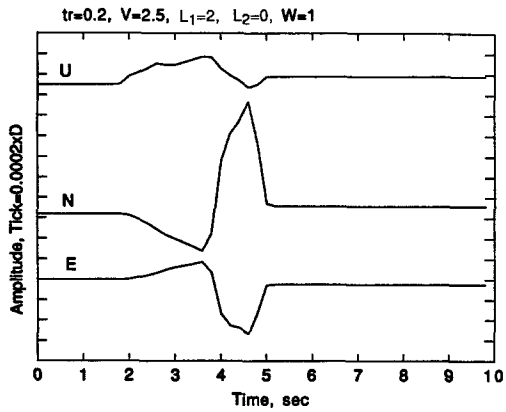

(a)

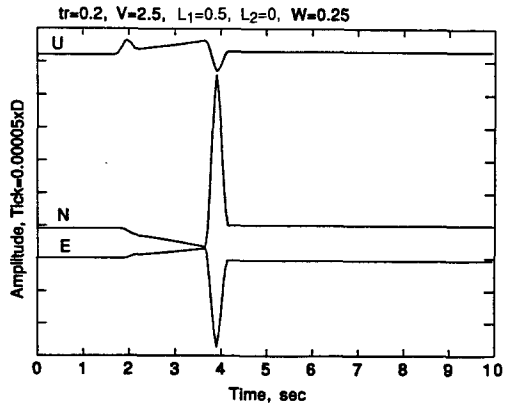

(b)

FIG. 2. Synthetic near-field displacements for a fault with an area of 2×1 km^2 (a), and 0.5×0.25 km^2 (b).

used for modeling of the far-field displacement. The moment value determined from the far-field pulses should be taken as the lower bound.

Although the above model explains the amplitude of the near-field displacement, it produces far-field pulses which are too wide. The narrow far-field pulse observed in the data clearly suggests that the dimension of the rupture plane that gave rise to the far-field pulses is much smaller than that used in the above model. For example, as shown in Figure 2b, if we reduce the fault length and width to 0.5 and 0.25 km, respectively, we can explain the width of the far-field pulse. Although we cannot determine the detailed geometry of the source, the narrow far-field pulse requires a rupture dimension of 0.5 km or less. Since we observed two pulses, we need two such patches (asperities) to explain the far-field pulses. From the seismic moment determined from the far-field pulses, we obtain the displacement on these patches to be about 150 cm. However, if the moment release took place from only these two patches, we cannot explain the amplitude of the near-field displacement. This observation together with the discrepancy between the seismic moments determined from the far-field and near-field suggests that some moment release took place from the region surrounding the two patches. This moment release must have taken place somewhat more slowly than that responsible for the far-field pulses. The overall fault dimension cannot be determined, but in view of the extent of the aftershock area, it appears to be at least 2 km.

Conclusion

Although the observation was at only one site, the short-range broadband data could resolve the rupture pattern with a spatial resolution of less than 1 km. Since the seismic moments and the upper bound of the rupture area from which the far-field pulse was generated are well determined, we can estimate the stress drop associated with this earthquake. Figure 3 shows the relation between the fault area

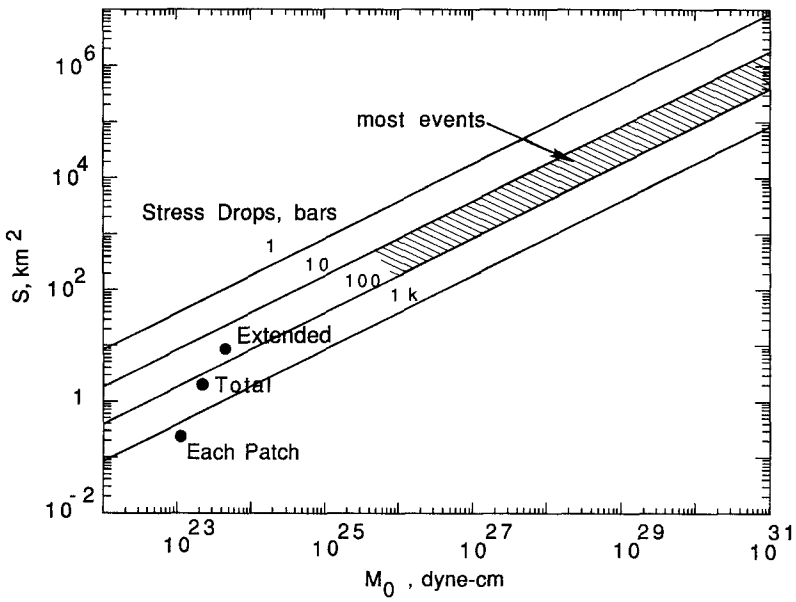

FIG. 3. The relation between the fault area, S, and the seismic moment, M_0, for different stress drops. Three stress-drop estimates for the Pasadena earthquake are shown.

and the seismic moment with the stress drop as a parameter. As shown by many investigators (e.g., Aki, 1972; Kanamori and Anderson, 1975), most large earthquakes plot between the lines for $\Delta\sigma = 10$ and 100 bar. For the Pasadena earthquake, we obtained $M_0 = 1.2 \times 10^{23}$ dyne-cm ($\frac{1}{2}$ of the seismic moment determined from the far-field pulse) and $S = 0.25$ km^2 (upper limit) for each asperity (patch), which leads to a stress drop larger than 2 kbar. Even if we allow for the uncertainties involved in the source parameter determinations, this conclusion appears inescapable. If we use the total moment obtained from the far-field data and $S = 2$ km^2 (estimate from the immediate aftershock area), the stress drop is approximately 200 bar. The total aftershock area shown in Figure 2 of Jones *et al.* (1989) is about 4 km long. If we assume an aspect ratio of 2 for the extended fault plane, the area of the extended fault plane is 8 km^2. If we assume that the total seismic moment obtained from the near-field data (4.6×10^{23} dyne-cm) is released from this area, the stress drop is about 50 bars.

Thus, the Pasadena earthquake provided evidence that the fault zone here, even at a depth of 15 km, has strong spots (asperities) that can sustain stresses of an order of 1 kbar.

ACKNOWLEDGMENTS

We thank Lucy Jones and Harold Magistrale for the information on the location and the first-motion mechanism of this event. This research was partially supported by the USGS Grant 14-08-0001-G1354. Contribution number 4806, Division of Geological and Planetary Sciences, California Institute of Technology, Pasadena, California.

REFERENCES

Aki, K. (1972). Earthquake mechanism, *Tectonophysics* **13,** 423–446.

Given, D. D., L. A. Wald, L. M. Jones, and L. K. Hutton (1989). The southern California Network Bulletin July–December 1987, *U. S. Geol. Surv., Open-File Rept. 89-323*, 2–3.

Haskell, N. A. (1969). Elastic displacements in the near-field of a propagating fault, *Bull. Seism. Soc. Am.* **59,** 865–908.

Jones, L. M., K. E. Sieh, E. Hauksson, and L. K. Hutton (1989). The 3 December 1988, Pasadena, California, Earthquake: evidence for strike-slip motion on the Raymond fault, *Bull. Seism. Soc. Am.* **80,** 474–482.

Kanamori, H. (1989). Pasadena very-broad-band system and its use for real-time seismology, extended abstract for the U.S.–Japan Seminar on Earthquake Prediction, Morro Bay, California, September 12–15, 1988, *U. S. Geol. Surv. Open-File Rept. 90-98.*

Kanamori, H., and D. L. Anderson (1975). Theoretical basis of some empirical relations in seismology, *Bull. Seism. Soc. Am.* **65,** 1073–1095.

Steim, J. M. (1986). The Very-Broad-Band Seismograph, *Ph.D. Thesis*, Harvard University, Cambridge, Massachusetts.

Wielandt, E. and G. Streckeisen (1982). The leaf-spring seismometer: design and performance, *Bull. Seism. Soc. Am.* **72,** 2349–2367.

SEISMOLOGICAL LABORATORY
CALIFORNIA INSTITUTE OF TECHNOLOGY
PASADENA, CALIFORNIA 91125
(HK)

UNITED STATES GEOLOGICAL SURVEY
525 SOUTH WILSON AVENUE
PASADENA, CALIFORNIA 91106
(JM, THH)

Manuscript received 12 October 1989